ISSN 1674-1056
http://cpb.iphy.ac.cn
http://iopscience.iop.org/cpb
中国物理 B
Chinese Physics
中国物理
Chinese Physics B

# Metamaterials and metasurfaces for designing metadevices: Perfect absorbers and microstrip patch antennas

Yahong Liu(刘亚红), Xiaopeng Zhao(赵晓鹏)

**Citation:**Chin. Phys. B . 2018, 27(11): 117805. **doi:** 10.1088/1674-1056/27/11/117805

Journal homepage: http://cpb.iphy.ac.cn; http://iopscience.iop.org/cpb

**What follows is a list of articles you may be interested in**

---

## High-performance lens antenna using high refractive index metamaterials

Lai-Jun Wang(王来军), Qiao-Hong Chen(陈巧红), Fa-Long Yu(余发龙), Xi Gao(高喜)

Chin. Phys. B . 2018, 27(8): 087802. **doi:** 10.1088/1674-1056/27/8/087802

## Controlling flexural waves in thin plates by using transformation acoustic metamaterials

Xing Chen(陈幸), Li Cai(蔡力), Ji-Hong Wen(温激鸿)

Chin. Phys. B . 2018, 27(5): 057803. **doi:** 10.1088/1674-1056/27/5/057803

## Design and theoretical study of a polarization-insensitive multiband terahertz metamaterial bandpass filter

Hai-Peng Li(李海鹏), Wen-Yue Fu(付文悦), Xiao-Peng Shen(沈晓鹏), Kui Han(韩奎), Wei-Hua Wang(王伟华)

Chin. Phys. B . 2017, 26(12): 127801. **doi:** 10.1088/1674-1056/26/12/127801

## Modeling for multi-resonant behavior of broadband metamaterial absorber with geometrical substrate

Kai-Lun Zhang(张凯伦), Zhi-Ling Hou(侯志灵), Song Bi(毕松), Hui-Min Fang(房惠敏)

Chin. Phys. B . 2017, 26(12): 127802. **doi:** 10.1088/1674-1056/26/12/127802

## Guided mode resonance in planar metamaterials consistingof two ring resonators with different sizes

Zhen Yu(俞禛), Hang Che(陈航), Jianjun Liu(刘建军), Xufeng Jing(井绪峰), Xiangjun Li(李向军), Zhi Hong(洪治)

Chin. Phys. B . 2017, 26(7): 077804. **doi:** 10.1088/1674-1056/26/7/077804

---

TOPICAL REVIEW — 80th Anniversary of Northwestern Polytechnical University (NPU)

# Metamaterials and metasurfaces for designing metadevices: Perfect absorbers and microstrip patch antennas*

Yahong Liu(刘亚红) and Xiaopeng Zhao(赵晓鹏)†

*Smart Materials Laboratory, Department of Applied Physics, Northwestern Polytechnical University, Xi'an* 710129, *China*

(Received 17 July 2018; revised manuscript received 19 September 2018; published online 8 October 2018)

In the past twenty years, electromagnetic metamaterials represented by left-handed metamaterials (LHMs) have attracted considerable attention due to the unique properties such as negative refraction, perfect lens, and electromagnetic cloaks. In this paper, we present a comprehensive review of our group's work on metamaterials and metasurfaces. We present several types of LHMs and chiral metamaterials. As a two-dimensional equivalent of bulk three-dimensional metamaterials, metasurfaces have led to a myriad of devices due to the advantages of lower profile, lower losses, and simpler to fabricate than bulk three-dimensional metamaterials. We demonstrate the novel microwave metadevices based on metamaterials and metasurfaces: perfect absorbers and microwave patch antennas, including novel transmission line antennas, high gain resonant cavity antennas, wide scanning phased array antennas, and circularly polarized antennas.

**Keywords:** left-handed metamaterials, chiral metamaterials, metasurfaces, perfect absorbers, microstrip patch antennas

**PACS:** 78.67.Pt, 81.05.Xj, 94.20.ws, 84.40.–x **DOI:** 10.1088/1674-1056/27/11/117805

## 1. Introduction

Left-handed metamaterials (LHMs) are artificial subwavelength periodic structure with negative permittivity and negative permeability simultaneously.[1–4] These materials were theoretically predicted in 1967 by Veselago.[1,2] In 1996 and 1999, Pendry demonstrated that wires and split resonant rings (SRRs) could achieve negative permittivity and negative permeability, respectively.[3,4] In the past twenty years, LHMs have become one of the research hotspots in the scientific community due to the unique properties such as negative refraction,[5] perfect lens,[6] and electromagnetic cloaks.[7,8] The first LHMs were proposed and experimentally verified in the microwave frequency by Shelby *et al.*[5] From then on, many types of LHMs at microwave, terahertz, and optical frequency have been proposed,[9–39] such as fishnet structure LHMs,[9] H-shaped LHMs,[10] S-shaped LHMs,[11] omega-shaped LHMs,[12] hexagonal-shaped LHMs,[13] and dendritic LHMs.[14–17] However, it is a challenge to achieve three-dimensional bulk LHMs in infrared and optical frequencies by using the present micro-nano fabrication processes. Besides that, metamaterials suffer from high losses in these high frequencies. Therefore, it is particularly necessary to investigate high-quality and planar low-loss metamaterials in high frequency. Dolling *et al.*[21] prepared an Ag–$MgF_2$–Ag fishnet-structure LHM with a working wavelength of 780 nm. Moreover, dielectric-based LHMs have been designed to reduce losses. Zhao *et al.* proposed low-loss microwave ceramic LHMs.[22,23] Ginn *et al.*[24] proposed an all-dielectric structure, which can achieve negative permeability and negative permittivity in the mid-infrared frequency band.

The most prominent feature of LHMs is that they have negative refraction, which cannot be found in natural materials. Besides LHMs, Tretyakov[40] and Pendry[41] proposed that the chiral metamaterials (CMs) could exhibit strong negative refraction as circularly polarized (CP) wave propagates inside the CMs. In addition, CMs, as another class of artificial materials, are extremely appealing for achieving strong polarization rotation,[42,43] circular dichroism,[44,45] and even the prospect of a repulsive Casimir force.[46] Among these properties, polarization rotation is one of the basic properties of electromagnetic waves conveying valuable information in the fields of signal transmission and wireless communication.[47–57] Rogacheva *et al.*[47] proposed bilayered CMs with giant gyrotropy, which could rotate the polarization plane of a linearly polarized (LP) wave propagating through it. Grady *et al.*[49] demonstrated ultrathin, broadband, and highly efficient metasurface-based polarization converters that are capable of rotating a linear polarization state into its orthogonal one. We proposed several broadband CMs with negative refractive index and large polarization rotation.[50–53] Moreover, we have designed CMs-based devices by using our proposed CMs, such as 90°-polarization rotation devices and circularly

*Project supported by the National Natural Science Foundation of China (Grant Nos. 11674267, 51272215, 11874301, and 11204241), the National Basic Research Program of China (Grant No. 2012CB921503), the National Aerospace Science Foundation of China (Grant No. 2016ZF53061), the Fundamental Research Funds for the Central Universities, China (Grant No. 3102017jghk02004), and the Natural Science Basic Research Plan in Shaanxi Province of China (Grant No. 2017JM1009).

†Corresponding author. E-mail: xpzhao@nwpu.edu.cn

© 2018 Chinese Physical Society and IOP Publishing Ltd 

polarized antennas.[54–57]

Although LHMs and CMs have mysterious electromagnetic and optical properties, they are three-dimensional bulk metamaterials, and it is difficult to prepare them, especially in the high frequency. In the last few years, as the two-dimensional equivalent of three-dimensional bulk metamaterials, metasurfaces have been a research hotspot because they are lower profile, lower losses, and simpler to fabricate than bulk metamaterials.[58–114] In 2011, Yu *et al.*[59] first proposed a V-shaped nanoantenna-array metasurface, which could provide abrupt phase discontinuities for light propagating through the interface and drastically change the flow of reflected and refracted light. Metasurfaces have the exceptional electromagnetic abilities including light bending,[59] beam focusing,[60] circular polarizers,[61] anomalous refraction and reflection, and flat lenses[63] across subwavelength thicknesses. Sun *et al.*[64] demonstrated theoretically and experimentally that a specific gradient index metasurface converted a propagating wave to a surface wave with nearly 100% efficiency. Pfeiffer *et al.*[65] proposed Huygens' surfaces that could redirect an incident beam with high efficiency into a refracted beam. Very recently, Ra'di[66] demonstrated that graded metasurfaces can achieve beam steering in reflection with unitary efficiency. Following that, broadband high-efficiency metasurfaces[67–70] have been proposed successively.

However, these metal-based metasurfaces suffer from detrimental effects of absorption, heating, and higher losses. Therefore, metal–dielectric hybrid metasurfaces and all-dielectric metasurfaces[71–76] have attracted a lot of attention. Guo *et al.*[73] investigated a hybrid metasurface composed of metal–dielectric nanoantennas that directed light from an incident plane wave or from localized light sources into a preferential direction. Zhan *et al.*[74] proposed a dielectric low-loss metasurface, which could generate a vortex beam. Ma *et al.*[75] demonstrated an all-dielectric metasurface operating in the terahertz band that was capable of engineering a reflected beam's spatial properties with high efficiency.

Progress in metasurfaces has led to a myriad of metadevices. It is demonstrated that metasurfaces have a wide range of applications in the fields of absorbers, novel antennas, lens, and wireless communications. Among these metasurfaces-based applications, a lot of works focus on novel perfect absorbers. For instance, Cole *et al.*[77] proposed an all-dielectric metasurface consisting of a dielectric cylinder embedded in a low index material that can act as a perfect terahertz absorber. Kang *et al.*[78] designed a dipole-like metasurface, having coherent perfect absorptions in any polarizations. Song *et al.*[79] proposed a water-resonator-based metasurface with a near-unity electromagnetic absorption. Recently, some active[80] and multifunctional[81] metasurfaces have been designed, which can be electronically switched between reflection, cross-polarization conversion, and high absorption. Another interesting application is that metasurfaces can be implemented to manipulate the radiation of electromagnetic waves and can be used to design novel microwave antennas. Wan *et al.*[84] designed a transformational metasurface Luneburg lens, which had a very good performance in controlling the radiated surface waves. Chen *et al.*[85] proposed non-Foster, negatively capacitive metasurfaces, which could be employed to design broadband ultrathin cloaks. The proposed active cloak may impact not only invisibility and camouflaging, but also practical antenna and sensing applications. Germain *et al.*[86] designed a phase-compensated metasurface which could be used as a reflector in a conformal Fabry–Pérot resonant cavity. The results showed that it could produce a directive emission in the desired direction. Li *et al.*[81,82] demonstrated that linear-to-circular polarization conversion focusing metasurface can be used to design circularly polarized high-gain antenna. We have proposed and experimentally demonstrated several types of metasurfaces-based antennas,[56,57,87–98] including more directional linearly polarized antennas, circularly polarized antenna, and omnidirectional antenna.

The aim of the paper is to present a comprehensive review of our group's work on metamaterials and metasurfaces. Besides, we also summarize some microwave metadevices based on metamaterials and metasurfaces. This paper is organized as follows. In Section 2, several typical microwave metamaterials and metasurfaces are introduced. In Section 3, we present broadband perfect absorbers based on metamaterials and metasurfaces. Some new novel microwave antennas are displayed in Section 4. The conclusion and outlook are given in Section 5.

## 2. Metamaterials and metasurfaces

### 2.1. Several LHMs

In this section, we briefly describe several typical LHMs which are proposed by our group,[119–129] including LHMs consisting of hexagonal SRRs and wires,[13,119–133] bowknot-shaped LHMs,[124] and dendritic-shaped LHMs.[14–17,125,126] Figure 1(a) shows the LHMs consisting of hexagonal SRRs and wires. The hexagonal SRRs produce magnetic resonance and the wires produce electric resonance.[13] Figure 1(b) presents the bowknot-shaped LHMs,[124] which can produce the two resonant modes of magnetic resonance and electric resonance at the parallel incidence (wave vector $k$ along $X$-axis) and normal incidence (wave vector $k$ along $Y$-axis), respectively. As presented in Fig. 1(c),[124] the two resonant modes appearing overlapped in the II region will lead to the negative index behavior. Moreover, the negative index frequency band can be tailored at three different regions of I, II, and III by changing the parameters of the bowknot unit cell.

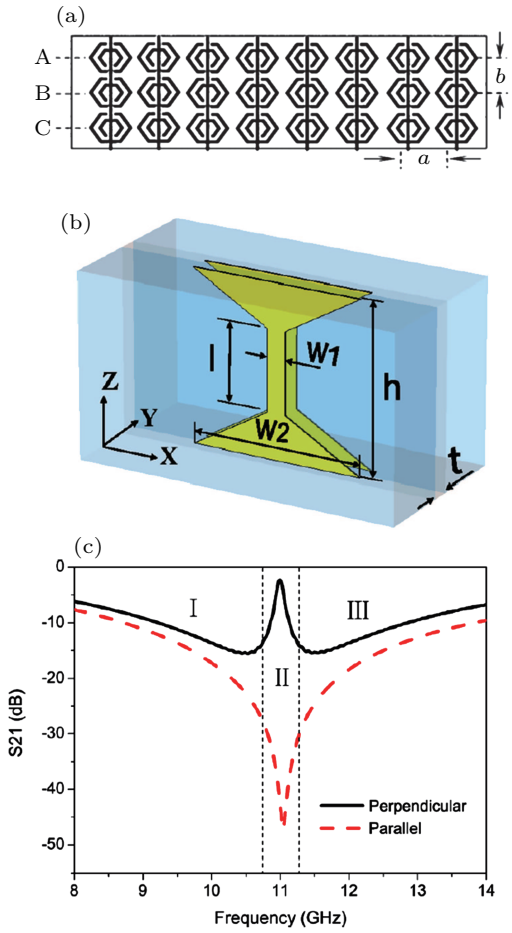



**Fig. 1.** (color online) (a) LHMs consisting of hexagonal SRRs and wires. (b) Bowknot-shaped LHMs, and (c) the transmission spectra, wave vector $k$ is along $X$-axis and $Y$-axis for the parallel and normal incidences, respectively.[124]

One of the most representative LHMs proposed by our group is dendritic structure LHMs as shown in Fig. 2.[15] The unitary dendritic structure displayed in Fig. 2(a) can provide overlapping negative permittivity and negative permeability at a resonant frequency band. Figures 2(b) and 2(c) display the electric and magnetic resonant modes. As shown in Fig. 2(b), in this mode, the positive and negative charges distribute on the two ends of the dendritic structure along the electric field direction. The resonance is similar to wires, producing an electric resonance. Figure 2(c) is the second resonant mode, which shows that the dendritic unit cell can be regarded as four coupled SRRs, producing a magnetic resonance. Figure 2(d) shows the transmission spectra and retrieved effective parameters of the dendritic LHMs.

As compared with previously proposed LHMs, our proposed bowknot-shaped LHMs and dendritic-shaped LHMs have the advantages of simple structure and easy fabrication since we can use one metallic pattern as a unit cell to realize negative permittivity and negative permeability simultaneously. Therefore, it can be expected that the proposed LHMs may be convenient for applications.

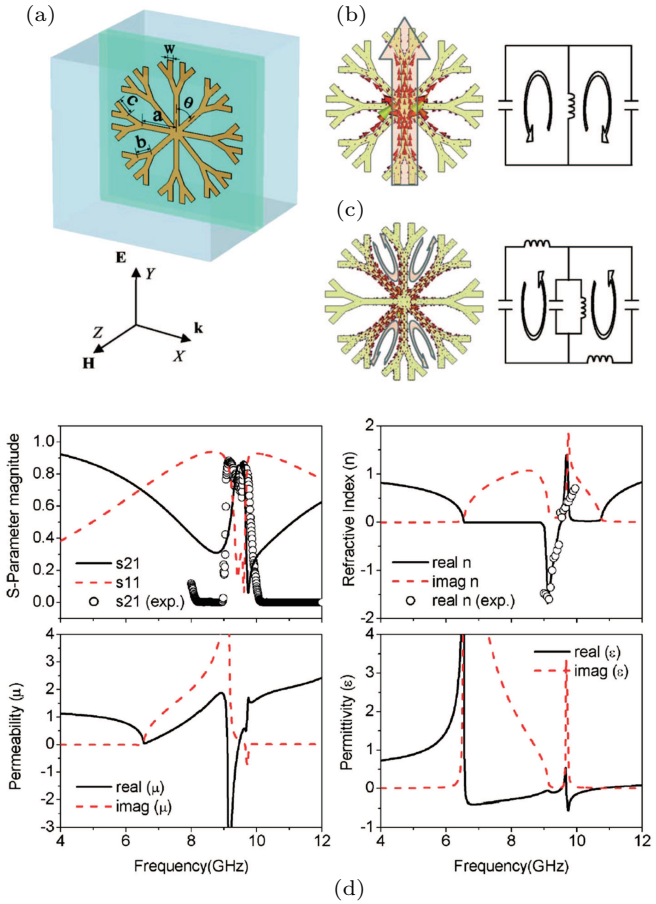



**Fig. 2.** (color online) (a) Unit cell of the dendritic LHMs. Surface current distributions of (b) the electric and (c) magnetic resonant modes. (d) Transmission spectra and retrieved effective parameters.[15]

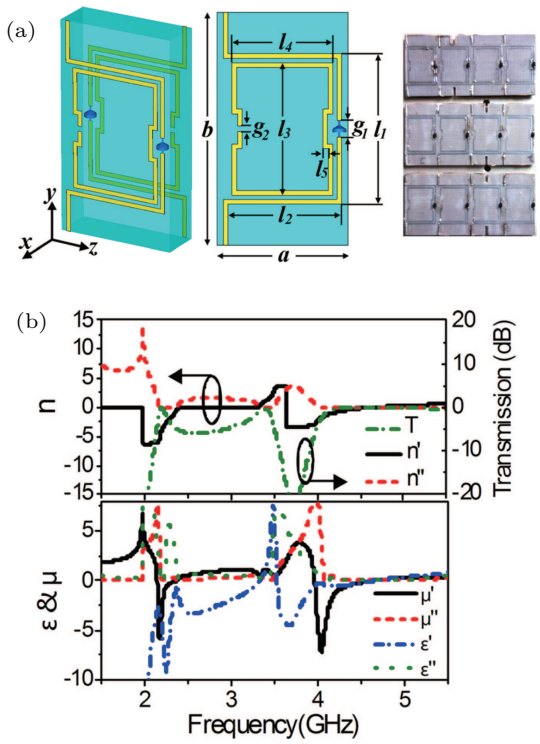



**Fig. 3.** (color online) (a) Schematic view of a unit cell of the DNLHM, (b) transmission spectra and retrieved effective parameters.[130]

Besides that, we also investigate dual bands and broadband LHMs.[121,122,130] Figure 3(a) displays our designed

dual-band nonlinear left-handed metamaterial (DNLHM).[130] The DNLHM operates at two left-handed bands where the refractive index is both negative. As presented in Fig. 3(b), the transmission coefficient and retrieved effective parameters show two left-handed transmission bands appearing at the center frequencies of 2.15 GHz and 4.3 GHz, where the real parts of the refractive index, permittivity, and permeability are simultaneously negative.

### 2.2. Broadband polarization rotation chiral metamaterials

LHMs have become hot topics due to the negative refraction. Besides LHMs, it is demonstrated that CMs can also have negative refractive index characteristics. Moreover, CMs have giant polarization rotation power which is several orders of magnitude larger than that of natural materials. However, resonance-based CMs suffer from highly dispersive polarization rotation and high losses at the resonant frequencies. Therefore, it is a challenge to design broadband nondispersive polarization rotation CMs with high transmission.

Figures 4(a) and (b) show two planar composite chiral metamaterials (CCM-1 and CCM-2) proposed by our group.[52,53] The two CCMs can achieve broadband dispersionless polarization rotation and high transmission simultaneously. Figure 4(c) depicts the results of the CCM1, which shows that the high transmission over 0.85 can be observed at the broadband frequency of 10.4–15.8 GHz. The ellipticity $\eta$ is approximately zero in the broadband frequency, revealing that the CCM-1 can realize pure polarization rotation in this region without distortion of polarization states. The similar results can also be obtained for the CCM-2.

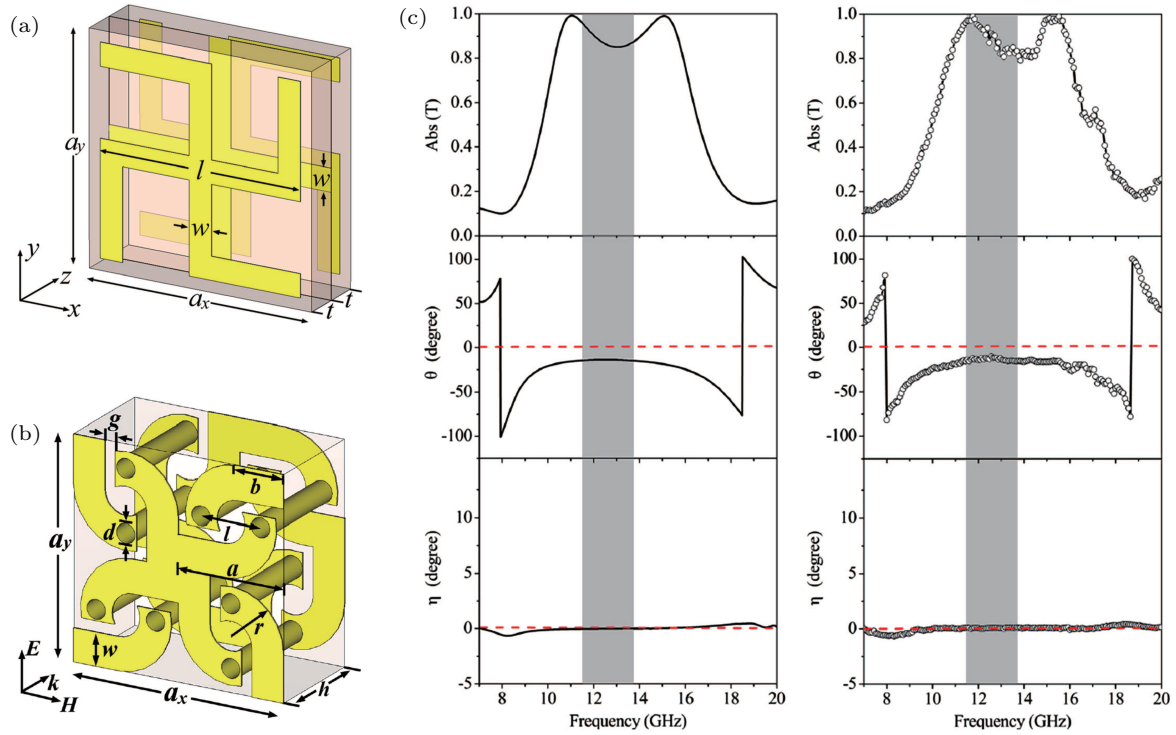



**Fig. 4.** (color online) Units cell of the designed (a) CCM-1[52] and (b) CCM-2.[53] (c) Simulation (left column) and measured (right column) results of the CCM-1.[52]

### 2.3. Circular-polarization-selective transmission based on a chiral waveguide

As an important subset of metamaterials, CMs present numerous fascinating properties. Recently, it has been demonstrated that CMs can accomplish asymmetric transmission[131,132] for the linearly polarized waves.[133,134] Here, based on chiral structure, we have designed and fabricated a chiral helical tape waveguide (CHTW), which can achieve a strong asymmetry between the orthogonal circular polarizations of transmitted electromagnetic wave.[55]

The configuration and the dimensions of the CHTW are shown in Fig. 5(a). Figure 5(b) presents the transmissions and reflections for circularly polarized (CP) incident waves, which shows a very high transmission of nearly 100% at a broadband frequency range whereas the reflection is very small for the right-handed circularly polarized (RCP) wave. Interestingly, when left-handed circularly polarized (LCP) wave is incident on the CHTW, the transmission is low where the reflection is also small. Figures 5(c) and 5(d) display the electric field distributions of the CHTW. It can be observed that little radiation occurs for RCP incident wave, resulting in a very high transmission. However, a significant leaky radiation occurs for LCP incident case, and the leaky radiation forms an interesting vortex. Therefore, a low transmission is observed for LCP wave. It can be expected that the CHTW can be used to distinguish the circular handedness of incident electromagnetic wave.

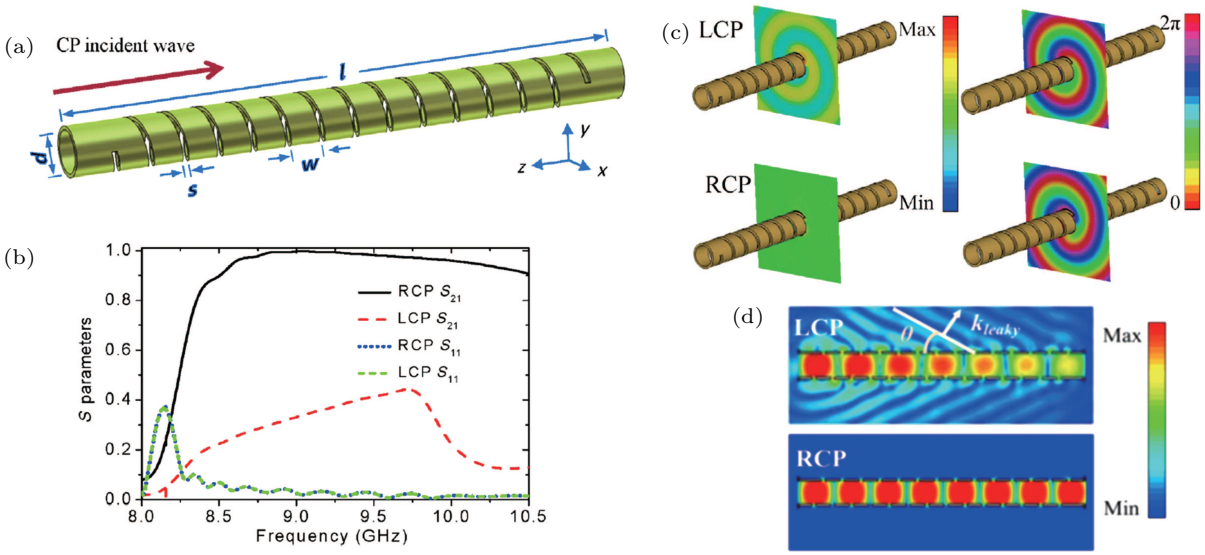



**Fig. 5.** (color online) (a) Schematic diagram of the proposed CHTW, (b) simulated transmissions $S_{21}$ and reflections $S_{11}$, (c) electric field intensity (right) and phase distributions (left) at $z = 0$ plane at 9 GHz, and (d) electric field intensity distributions at $x = 0$ plane at 9 GHz.[55]

### 2.4. Gradient phase discontinuity metasurfaces

Metasurfaces comprise a class of the two-dimensional equivalent of metamaterials which have subwavelength textured surfaces and can impart discontinuities on electromagnetic wavefronts. Compared with bulk three-dimensional metamaterials, metasurfaces have the merits of low loss, low weigh, and low profile. Here, we summarize gradient phase discontinuities metasurfaces proposed by our group.[76,135]

Figure 6 shows a gradient phase discontinuities metasurface based on chiral branched gammadion structure (CBGS),[135] consisting of eight CBGS unit cells for realizing a complete high transmission phase covered from $-180°$ to $+180°$ with $45°$ intervals at 10 GHz. The metasurface can refract a normally incident circular polarized wave to an angle at will by adjusting the geometric parameters of the CBGS. We demonstrate experimentally that the metasurface can refract a normally incident RCP wave to an angle of $17°$.

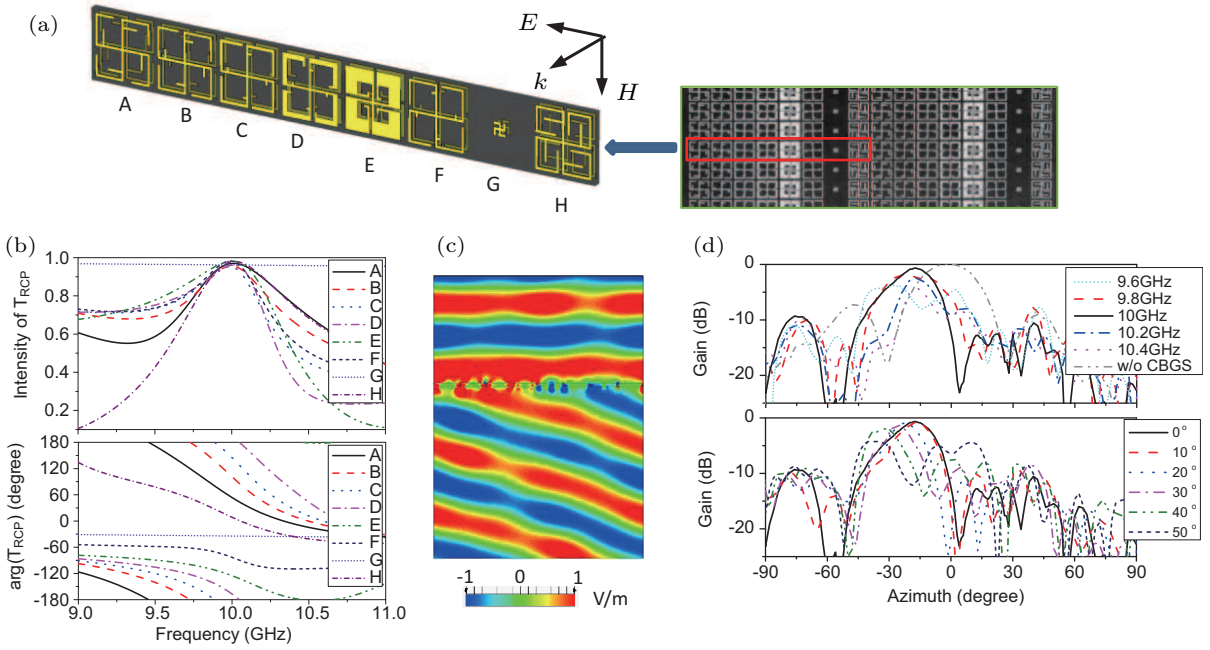



**Fig. 6.** (color online) (a) CBGS metasurface, (b) transmission intensity and transmission phase of each unit cell, (c) simulated electric field distribution of the refraction, and (d) measured far-field radiation patterns for various operating frequencies and incident angles.[135]

As compared with lossy metal-based metasurfaces, metal-dielectric hybrid metasurfaces and all-dielectric metasurfaces have lots of merits because they do not suffer from higher losses. Figure 7 is a broadband high-transmission gradient phase discontinuity metasurface consisting of cylindrical dielectric resonators (relative permittivity of $\varepsilon_r = 36.7$ and

$\tan\delta = 0.002$) and metallic wires.[76] One period of the designed metal–dielectric hybrid metasurface can achieve a complete transmission phase at a broadband frequency from 8 GHz to 9.8 GHz. It is shown that the metasurface can also refract a normally incident circular polarized wave to an angle at the broadband frequency.

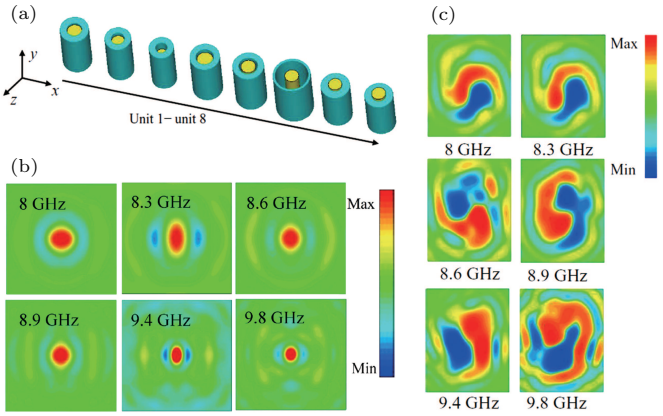



**Fig. 7.** (color online) (a) One period of the metal–dielectric hybrid metasurface. Simulated electric field distributions of the (b) focusing and (c) vortex at different frequencies.[76]

In addition, we demonstrate the flexibility and utility of this present metal–dielectric metasurface to produce wavefocusing and vortex beam. The simulated electric field distributions of the wavefocusing are displayed in Fig. 7(b), which presents that the metasurface can focus the transmission wave tightly to a spot of the diameter of about $0.06\lambda$. Figure 7(c) presents the electric field distributions of the vortex at various frequencies, which shows that a clear vortex is observed.

## 3. Perfect absorbers

### 3.1. Perfect absorbers with dendritic cells

In our previous studies, we demonstrate dendritic-shaped LHMs. Here we show that the dendritic structure can be used to design perfect absorbers.[139–142] The perfect absorbers are composed of metal dendritic resonators, a dielectric substrate, and a continuous metal copper film. Figure 8(a) shows a single unit cell of our perfect absorbers.[139] When an electromagnetic wave is normally incident on the absorbers, the transmission is blocked off by the metal copper film. Thus, only the reflection needs to concern. Figure 8(b) shows that the measured absorptivity can be up to 95.5% at 10.26 GHz. Next,

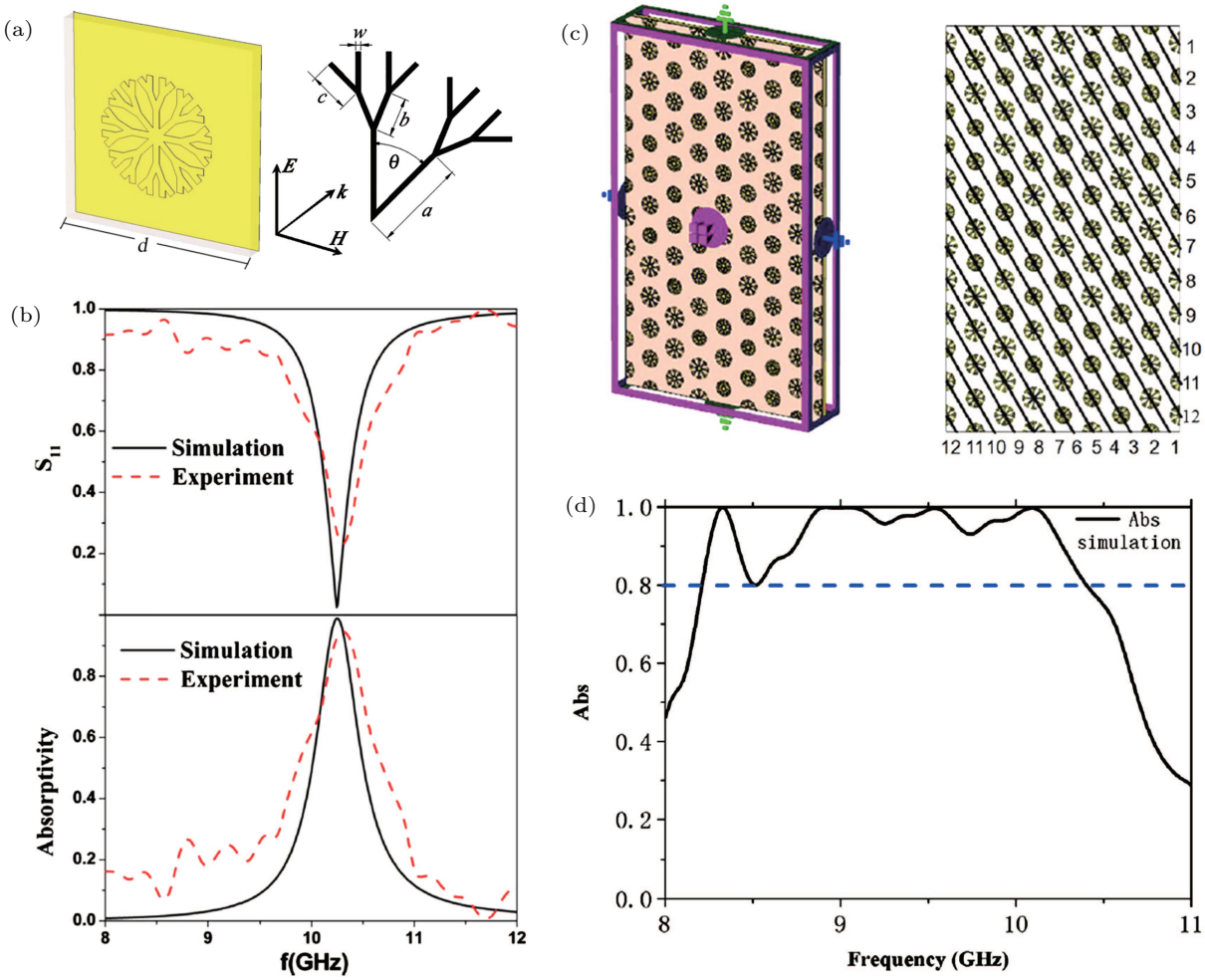



**Fig. 8.** (color online) (a) Unit cell of the perfect absorber, and (b) the reflection and absorption spectra.[139] (c) Prototype of the broadband perfect absorber, and (d) the absorption spectrum.[141]

we utilize dendritic structures with different sizes to enhance the absorption bandwidth. As known, each dendritic unit has a narrow bandwidth. In this case, we can design a broadband absorber consisting of 12 distinct dendritic unit cells as shown in Fig. 8(c). The absorption spectrum is shown in Fig. 8(d), which displays that a broadband absorption can be achieved.[141]

### 3.2. Dendritic structure perfect absorber based on resistance film

Compared to the broadband dendritic perfect absorber shown in Section 3.1, we propose a much more lightweight dendritic perfect absorber based on resistance film.[142] As shown in Figs. 9(a) and 9(b), the perfect absorber consists of three layers: copper film, polymethacrylimide (PMI) foam; and dendritic structures etched by indium-tin oxide (ITO) conductive film. Since surface resistivity structure is used instead of metal structures, the perfect absorber has a low weight. The experimental results are shown in Fig. 9(c), which presents that absorption is over 80% at the range of 8–17 GHz. Moreover, this perfect absorber is not sensitive to the incident angle.

### 3.3. Broadband perfect absorbers with circular patch cells

Genetic algorithms or multilayer structures are often used to design broadband metamaterial absorbers.[140,143] However, they are complicated and not easy to fabricate. In contrast to the narrow-band absorbers,[139,144] we propose an ultrathin broadband dendritic-based perfect absorber. Here we display another broadband perfect absorber as shown in Fig. 10, consisting of multiple circular metallic patches and a metallic ground plane separated by a single dielectric layer.[145] The absorption bandwidth can be broadened by increasing the number of multiple circular unit cells. As compared with the dendritic broadband perfect absorber, this perfect absorber has a simple structure, easy fabrication, and low cost.

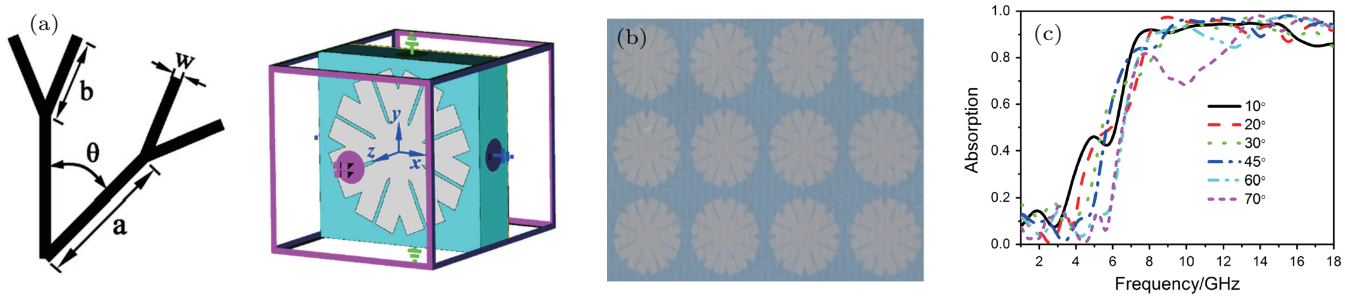



**Fig. 9.** (color online) (a) Unit cell of the perfect absorber based on resistance film, the parameters are shown as follows: $a = 1.8$ mm, $b = 2.6$ mm, $w = 1.2$ mm, $\theta = 45°$, $P = 10$ mm, $h = 3$ mm, $\varepsilon_r = 1.4$, and the surface resistance of the branch structure $r = 40\ \Omega/\square$. (b) Fabricated sample of the lightweight perfect absorber, and (c) the absoption spectra for different incident angles.[142]

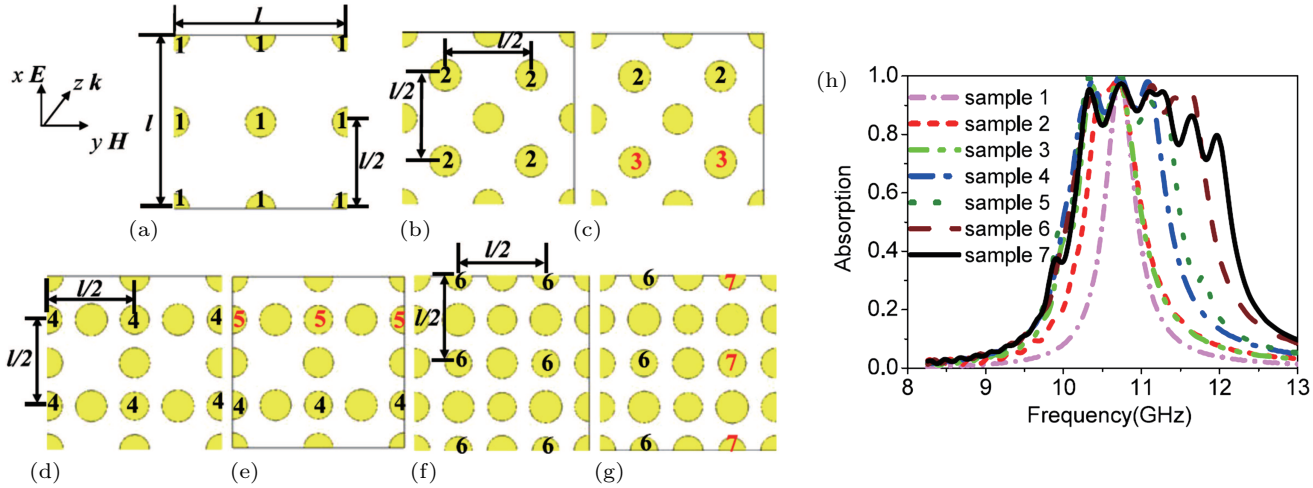



**Fig. 10.** (color online) Unit cell of the proposed absorbers: (a) sample 1, (b) sample 2, (c) sample 3, (d) sample 4, (e) sample 5, (f) sample 6, and (g) sample 7. (h) Absorption spectra for the different samples.[145]

### 3.4. Discussion

We use multiple unit cells with different geometric parameters to realize broadband absorbers. Increasing the numbers of unit cells can broaden the frequency range when their resonances are closely packed together, thereby resulting in a broadband resonance. In addition, the proposed absorbers can operate at a wide range of incident angles under both transverse electric and transverse magnetic polarizations. We propose a simple method to achieve broadband absorbers. According to the proposed theoretical model design method, broadband metamaterial absorbers based on other unit cells can also be obtained. The absorbers have potential applica-

tions in explosive detection, as well as in thermal detectors, cloaking, and other fields.

## 4. Novel microwave patch antennas

In this section, we present new novel microwave antennas based on metamaterials including the following four kinds of novel antennas: composite right/left-handed transmission line (CRLH-TL) microstrip patch antennas, high-gain patch antennas, steerable beam antennas, and circularly polarized patch antennas. For CRLH-TL antennas, we have designed low-cost and easy fabricated rectangular and circular patch antennas by using epsilon-negative transmission line (ENG-TL), respectively. The antennas can operate at two resonant frequencies and broadband frequencies according to optimized geometric parameters. Next, we present some high gain resonant cavity patch antennas. The gain of the patch antennas is enhanced drastically as compared with conventional patch antennas. And then, phased array antennas with a broadly steerable beam are demonstrated. Interestingly, the proposed phased array antennas have a much higher gain than conventional phased array antennas at the low elevation angles. Finally, we show a circularly polarized patch antenna based on chiral metamaterials. As known, a conventional method to construct a CP antenna needs to produce two degenerate orthogonal modes with equal amplitude and 90° phase difference on the radiating element. The feeding network complicates the CP antenna design and fabrication. A simple method for realizing a CP antenna by using chiral metamaterials is provided.

### 4.1. Microstrip patch antennas with CRLH-TL

CRLH-TL metamaterials have been originally demonstrated in the groups of Itoh, Oliner, and Eleftheriads,[146,147] respectively. CRLH-TL metamaterials are artificial composites consisting of a conventional TL loaded with series capacitors and shunt inductors,[148] and present some novel electromagnetic properties such as backward-wave radiation,[149] planar focusing,[150] and infinite wavelength.[151] It is demonstrated that CRLH-TL metamaterials can be used to design novel antennas.[152,153] Here, we summarize our proposed several microwave patch antennas based on CRLH-TL theory.[96–98,154]

#### 4.1.1. Rectangular patch antenna based on ENG FPOR

As one type CRLH-TL, ENG-TL has been implemented by just removing the series capacitance of CRLH-TL, which was first proposed by Lai and Park *et al.*[153–161] We have designed a low-cost and easy fabricated patch antenna by using ENG-TL. The proposed antenna is based on the ENG first-positive-order resonator (FPOR) with mushroom unit cells.[161] In order to demonstrate the performances of the ENG FPOR antenna, a conventional rectangular patch antenna A-1 is fabricated to compare with the FPOR antenna A-4, as shown in Fig. 11(a). Figure 11(b) displays the antenna reflections, which shows that antenna A-1 resonates at 9.58 GHz and A-4 works at 9.74 GHz. The measured far-field radiation patterns are displayed in Fig. 11(c), which shows that the gain of the ENG FPOR antenna is enhanced as compared with that of the conventional patch antenna.

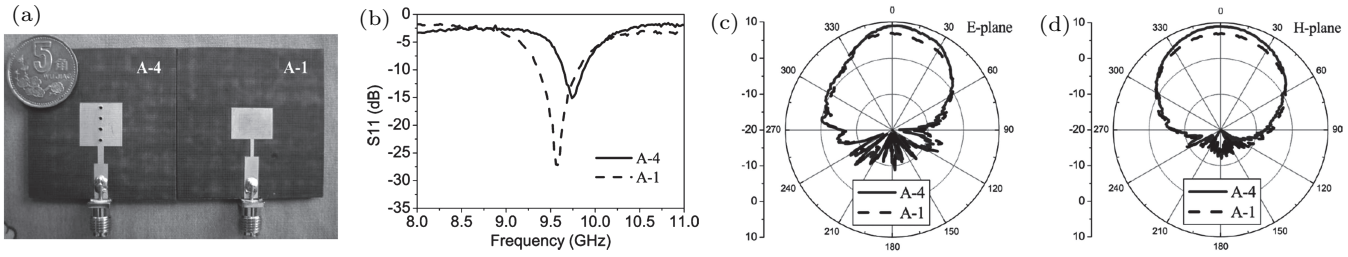



**Fig. 11.** (a) Fabricated antenna samples, (b) measured antenna reflections, and (c) far-field radiation patterns.[161]

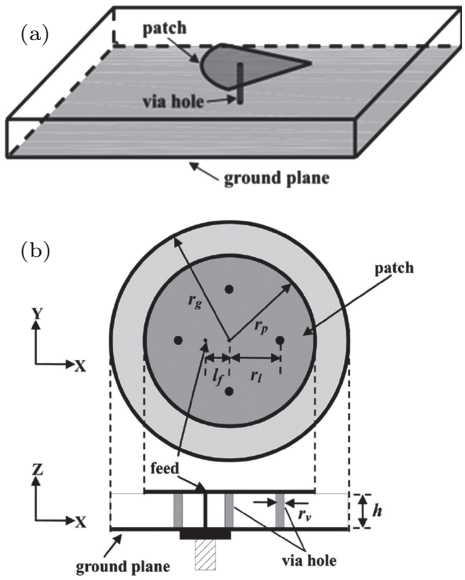
#### 4.1.2. Circular microstrip patch antennas based on ENG ZOR

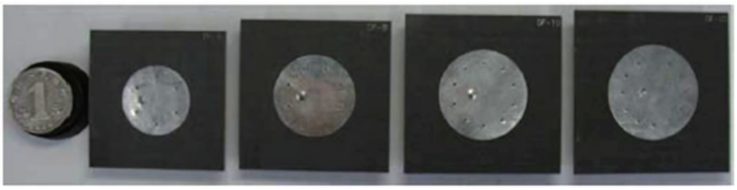
We have designed rectangular directional patch antenna based on ENG first-positive-order resonator (FPOR).[161] Some works demonstrate that rectangular ENG zeroth-order resonator (ZOR) antennas can realize omnidirectional radiation pattern, which are implemented by using the infinite wavelength property of the ENG-TL.[151,157,160] One of the most significant advantages is that the ENG ZOR antenna size/gain is independent of the resonant frequency. However, because the feed point is not at the center of the antenna, the radiation pattern is asymmetrical.

We have designed circular ENG patch antennas based on the ENG-TL.[96,97] The proposed antennas can demonstrate the characteristics of a monopole-type radiation pattern for dual-frequency.[96] Figure 12(a) shows a sectorial mushroom unit-cell consisting of a sectorial patch with a grounded via hole. By cascading the sectorial mushroom unit-cell $N$ times without gaps circularly periodically, a circular ENG ZOR could be realized, as shown in Fig. 12(b). In this antenna, the frequency of TM mode is not zero, but a finite value. Thus, it can be used as an operation mode with a monopole-type radi-

ation pattern. By matching the resistance, a higher mode can also be excited, and consequently, a dual-frequency antenna with monopole-type pattern can be achieved. We have designed four antennas (DF6, DF8, DF10, and DF12) as shown in Fig. 12(c).

Figure 13(a) shows the measured antenna reflections and farfield radiation patterns. Each antenna presents the first resonant peak around 5.25 GHz, and the second resonant frequency decreases with increasing $N$. All four antennas show similar radiation patterns. Figure 13(b) presents the radiation patterns of the antenna DF-8 as representative. Note that the antenna shows monopole-type radiation pattern at the two resonant frequencies.



| | DF-6 | DF-8 | DF-10 | DF-12 |
|---|---|---|---|---|
| $r_p$ (mm) | 13.00 | 15.20 | 16.83 | 18.10 |
| $r_g$ (mm) | 25.00 | 27.20 | 28.83 | 30.10 |
| $r_l$ (mm) | 8.80 | 10.55 | 11.70 | 12.55 |
| $r_v$ (mm) | 0.40 | 0.40 | 0.40 | 0.40 |
| $l_f$ (mm) | 5.45 | 4.80 | 4.70 | 4.55 |
| $\theta$ (deg.) | 60 | 45 | 36 | 30 |
| $N$ | 6 | 8 | 10 | 12 |

(c)

**Fig. 12.** (a) Configuration of a sectorial mushroom unit-cell, (b) circular ENG patch antenna, and (c) fabricated antennas DF-6, DF8, DF10, DF12.[96]

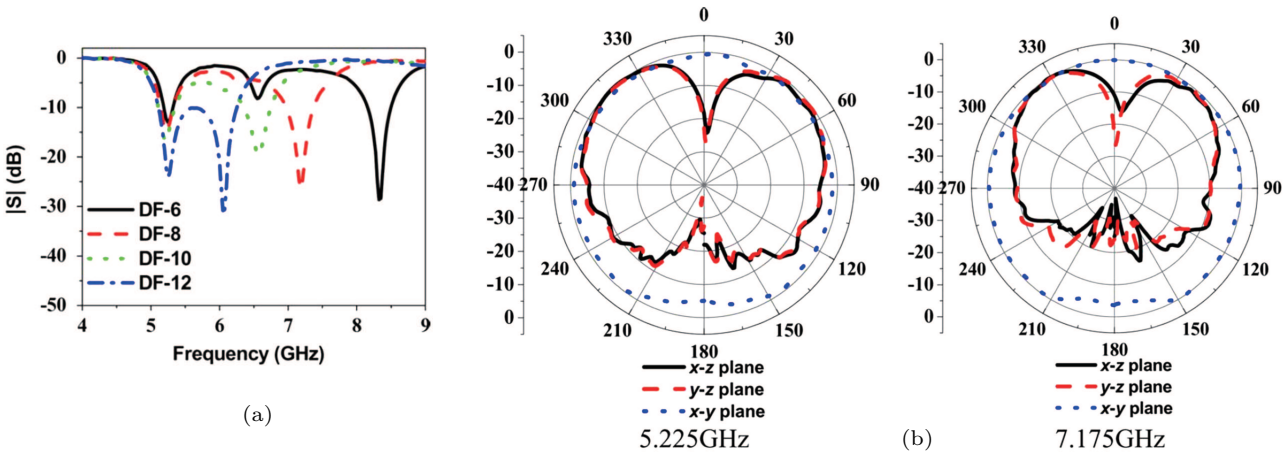



**Fig. 13.** (color online) Measured antenna (a) reflections and (b) far-field radiation patterns.[96]

### 4.2. High-gain patch antennas

#### 4.2.1. High-gain microstrip patch antenna with NPM

Microstrip patch antennas have the outstanding properties of low-profile and light-weight. It is shown that microstrip patch antennas are suitable for lots of applications. However, microstrip patch antennas also have some limitations of lower gain and narrow bandwidth. Metamaterials pave a new way to improve the performances of microstrip patch antennas.

We have designed a high-gain patch antenna by using anisotropic negative permeability metasurface (NPM).[87] Figure 14(a) schematically illustrates the radiation principle of the proposed antenna with anisotropic NPM cover. When the electromagnetic wave is incidence onto the NPM cover, the sideward radiation will be reduced and forward radiation can be enhanced, therefore the antenna gain is improved. The photographs of the conventional antenna and the NPM cover antenna are given in Fig. 14(b). Figure 14(c) presents the measured antenna reflections, which shows that the two antennas operate around 10 GHz. The measured far-field radiation patterns displayed in Fig. 14(d) show that the radiation of the NPM antenna is indeed focused to the forward direction and the antenna gain is enhanced drastically.

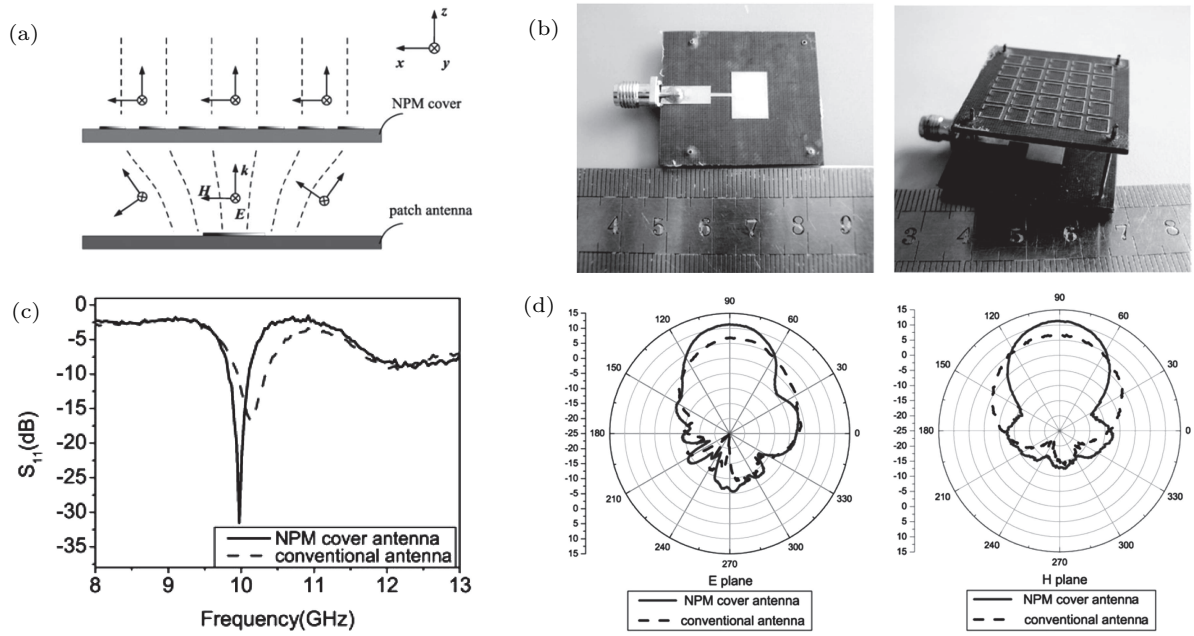



**Fig. 14.** (a) Radiation principle of the NPM cover antenna, (b) photographs of the fabricated antennas, (c) measured antenna reflections and (d) far-field radiation patterns.[87]

### 4.2.2. Ultrathin and high-gain resonant cavity antenna

Compared with NPM cover antenna as shown in Subsection 4.2.1, the much more ultrathin and high-gain resonant cavity antenna is presented. The antenna consists of the conventional single microstrip patch antenna and partially reflective surface (PRS), as shown in Figs. 15(a)–15(d).[88] Resonance condition of the antenna can be expressed as

$$h + d\sqrt{\varepsilon_{\rm r}} = (\Phi_{\rm PRS} + \theta_{\rm PEC})\frac{\lambda}{4\pi} + N\frac{\lambda}{2}.$$

It is shown that a significantly thin cavity thickness ($h$ = 0.5 mm) is achieved for $\phi_{\rm PRS} = -135°$.

Figures 15(e) and 15(f) show the antenna reflections and far-field radiation patterns, respectively. Antenna reflection curves show that the antenna resonates at 8.774 GHz. Notably, there are another two reflection peaks at 8.92 GHz and 9.13 GHz. However, from antenna point of view, the modes at the higher frequencies are not interesting, because they present multiple lobes in the radiation patterns. The measured maximum gain can be upto 13.2 dB at 8.774 GHz, which is much higher than that of the conventional microstrip patch antenna without PRS.

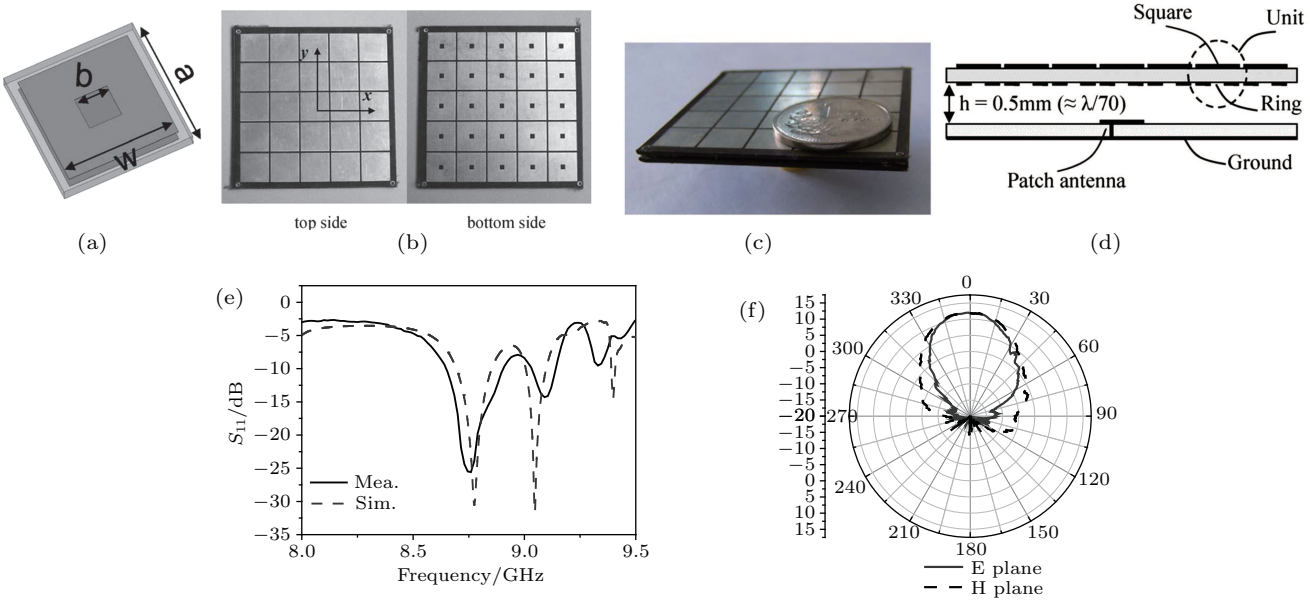



**Fig. 15.** (a) Unit cell of PRS, and (b) the fabricated PRS sample. (c) Photograph and (d) the schematic view of the proposed antenna. (e) Antenna reflection curves and (f) measured far-field radiation patterns.[88]

### 4.3. Phased array antennas with a steerable beam

It is shown that metamaterials have been used to realize beam-steerable antennas.[162–167] For instance, Chen *et al.*[162] theoretically analyzed that a controllable LHM could be used to realize a steerable antenna, with scanning capability in the range of $\pm 40^\circ$. Dhouibi *et al.*[163] proposed a planar metamaterial-based beam-scanning broadband microwave antenna, achieving beam-scanning with a coverage up to $120^\circ$. Pacheco *et al.*[164] designed an all-metallic steerable beam antenna using epsilon-near-zero metamaterials, with the antenna gain scan loss below 3 dB for angles up to $\pm 15^\circ$. In this section, we demonstrate phased array antennas based on zero index metamaterials (ZIMs) and gradient phase discontinuity metasurfaces.

#### 4.3.1. Wide scanning phased array antenna based on NZIMs

Near-zero-index metamaterials (NZIMs), as another type of metamaterials, have also become a vigorous topic of scientific research. We have designed broadband impedance-matched near-zero index metamaterials (BIMZIMs) consisting of a cylindrical dielectric resonator with a high-permittivity material and a thin metallic copper rod through the center of the cylindrical resonator, as displayed in Fig. 16(a). Retrieved index $n$, impedance $z$, permeability $\mu$, and permittivity $\varepsilon$ are displayed in Fig. 16(b), which shows that the real part of the index, $\mathrm{Re}(n)$, is near-zero over a broadband frequency range of 8.45–10.5 GHz and $\mathrm{Re}(n)$ equals to zero at 9 GHz.

It is demonstrated that the BIMZIMs have very interesting wave-manipulating properties at the frequencies where the refractive index is negative near-zero, zero, and positive near-zero. Based on the unique controlling wave characteristics, we propose a method for controlling the radiation of a phased array antenna by using the NZIMs.[92] For phased arrays, the grating lobes attain full amplitude when the critical scanning angle[164] is $\theta_{\mathrm{gc}} = \sin^{-1}\left(\frac{\lambda_0}{|n|d} - 1\right)$. If one can make metamaterials with $|n|$ less than 1, the critical scanning angle $\theta_{\mathrm{gc}}$ will be enhanced and grating lobes will be forbidden. We have constructed a phased array antenna with 11 antenna elements. As shown in Figs. 16(c)–16(f), the antenna grating lobe disappears as the BIMZIMs lens with $|n|$ less than 1 is used.

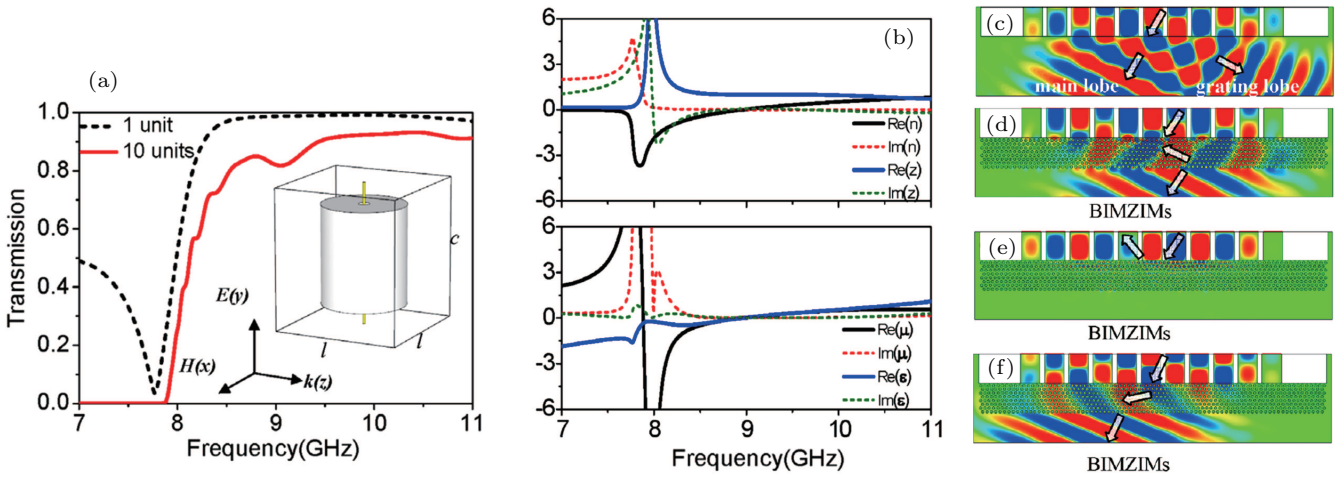



**Fig. 16.** (color online) (a) Transmission coefficients and (b) the retrieved index $n$, impedance $z$, permeability $\mu$, and permittivity $\varepsilon$. Simulated electric field intensity distributions for (c) the phased array antenna without the BIMZIMs lens, and (d)–(f) the phased array antenna with the BIMZIMs lens operating at (d) 8.6 GHz with index of negative near-zero, (e) 9 GHz with $n = 0$, and (f) 10 GHz with index of positive near-zero.[92]

#### 4.3.2. Broadly steerable beam antenna based on metasurface

We have demonstrated that NZIMs can offer unique grating conditions in a phased array antenna, with the beam scanning angle range beyond the critical angle limit of the grating lobes. Unlike the previously studied steerable beam antenna, we have designed a novel phased array antenna with a broadly steerable beam by using a gradient phase discontinuity metasurface.[93]

The designed metasurface shown in Figs. 17(a) and 17(b) can realize a gradient transmission phase and can refract the incident plane electromagnetic wave at an angle of $\theta_{\mathrm{t}} = 45^\circ$. As shown in Fig. 17(c), as a five-element equally spaced array has a zero progressive phase shift between elements, the beam direction is $0^\circ$. The maximum scanning angle is $\theta_{\mathrm{m}}$ when the array has an appropriate progressive phase shift between elements. For realizing a broadly steerable beam, the metasurface lens refracting electromagnetic wave to a certain angle $\theta_{\mathrm{t}}$ is employed to the array. As presented in Fig. 17(d), when covered with the metasurface lens, the array has a beam centered at $\theta_{\mathrm{t}}$, and the maximum scanning angle would be $\theta_{\mathrm{t}} + \theta_{\mathrm{m}}$. Figure 17(e) presents the antenna far-field radiation patterns, which shows that the main beam is $0^\circ$ and $45^\circ$ for the conventional phased antenna and the metasurface phased array antenna, respectively. The results show that the antenna main beam can be steered drastically. In addition, the proposed array antenna has a much higher gain than conventional phased array antennas at the low elevation angles.

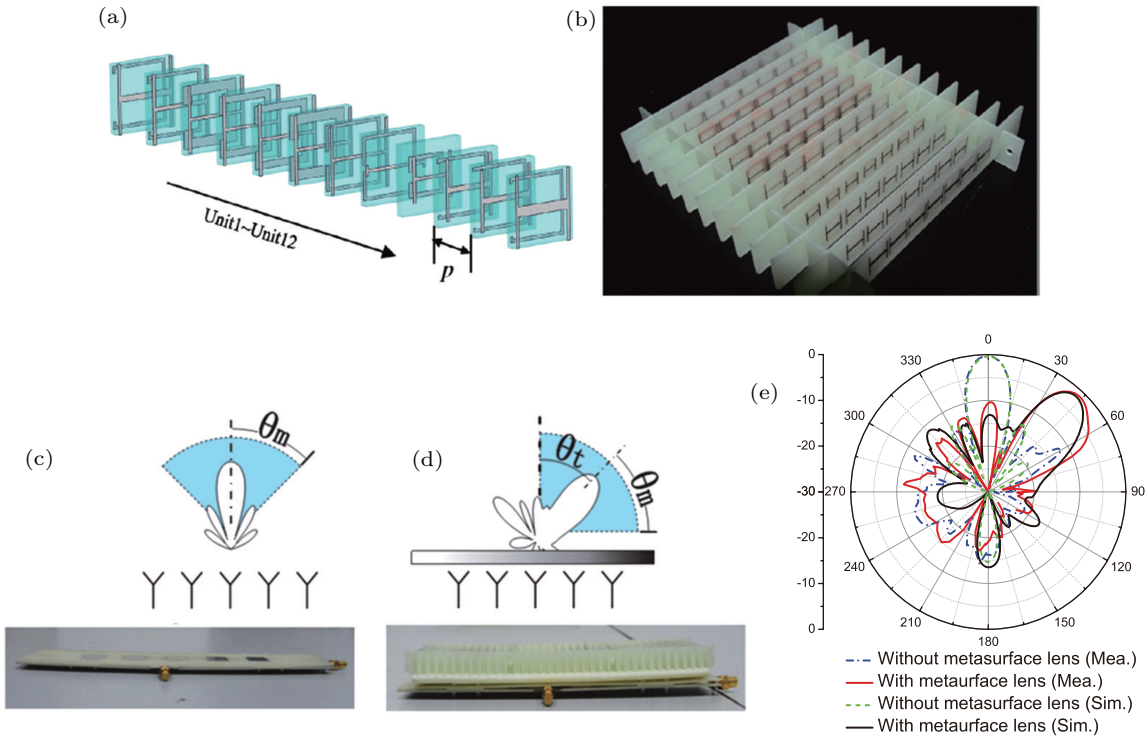



**Fig. 17.** (color online) (a) One period of metasurface, (b) fabricated metasurface lens, (c) conventional phased array antenna, (d) phased array antenna with the metasurface lens, and (e) far-field radiation patterns of the phased array antennas.[93]

### 4.4. Circularly polarized patch antenna with CMs

Chiral metamaterials have attracted great interests because of the unique properties of the negative refraction index, optical activity, circular dichroism, and asymmetric transmission. Based on these properties, novel microwave devices have been designed and fabricated. We propose an ultrathin controllable CM. Based on the polarization property of the proposed CM, a CP patch antenna is constructed.[56,57]

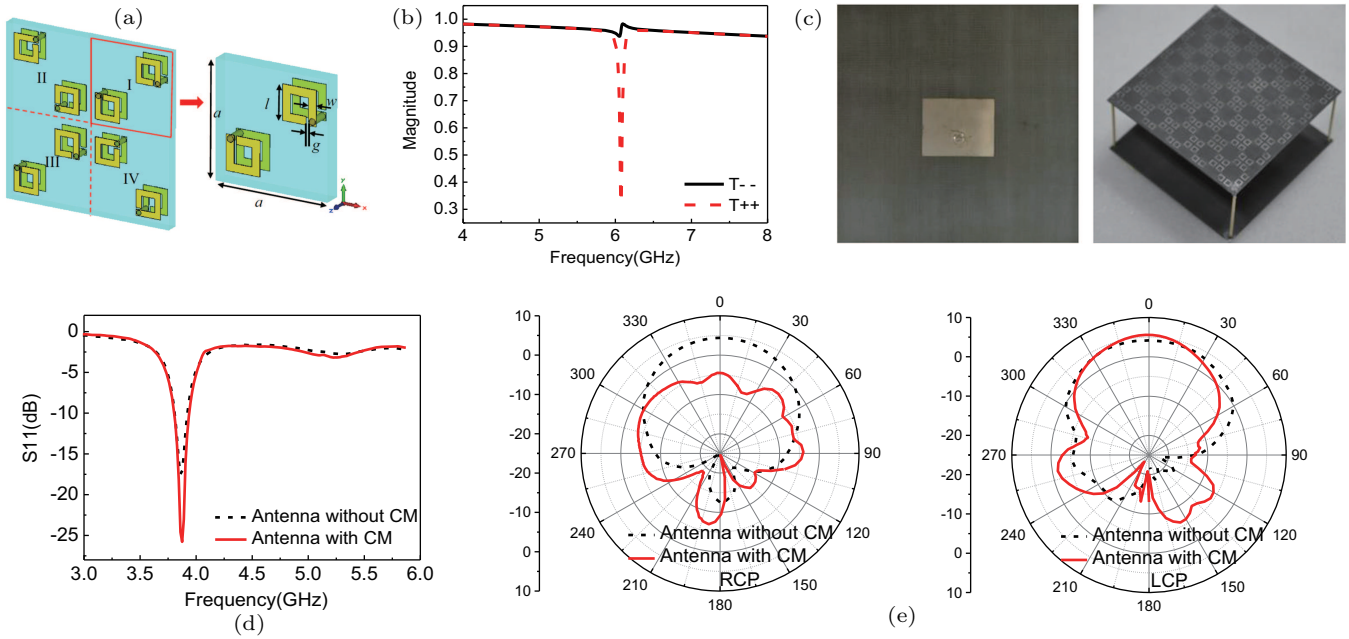



**Fig. 18.** (color online) (a) Unit cell of the proposed LCP CM. (b) Transmission of the proposed LCP CM. (c) Fabricated LP patch antenna and the LCP patch antenna. (d) Measured antenna reflections, and (e) far-field radiation patterns.[56]

Figure 18(a) shows a unit cell of the LCP CM consisting of four zones.[56] The simulated transmission spectra ($T_{++}$ and $T_{--}$) of the CM are depicted in Fig. 18(b), where $T_{++}$ and $T_{--}$ represent transmission of the RCP and LCP waves, respectively. It shows that $T_{--}$ is prominent and $T_{++}$ is little at 6.07 GHz. Based on the polarization characteristic of the proposed CM, a LCP patch antenna can be implemented, as shown in Fig. 18(c). Figures 18(d) and 18(e) present the

measured antenna reflections and far-field radiation patterns, which show that as the LCP CM is used, the measured antenna LCP gain is much higher than that of RCP. The result indicates that the antenna polarization mode is changed from LP mode to LCP mode. It can be expected that CMs will exploit an avenue for designing CP antennas.

## 5. Conclusion and outlook

In conclusion, we summarize several representative metamaterials and metasurfaces, which are designed by our group, such as LHMs, CMs, and gradient phase discontinuity metasurfaces. As compared with three-dimensional bulk metamaterials, metasurfaces have a reduced dimension and provide us new degrees of freedom to control the phase, amplitude, and polarization. Therefore, metasurfaces are more suitable for designing new microwave metadevices. With the unique properties of the metamaterials and metasurfaces, some interesting applications including broadband perfect absorbers and novel microwave antennas are presented in this paper.

Until now, several types of metasurfaces including multi-resonance metasurface,[59,168] Pancharatnam–Berry-phase metasurface,[99,169,170] Huygens' metasurface,[65,171,172] and all-dielectric metasurface[71–76,173–176] are proposed and investigated extensively.[177] Each metasurface has different advantages and limitations. Multi-resonance metasurface is proposed firstly, such as the well-known metasurface consisting of V-shaped antennas.[59] Since ordinary and anomalous reflection/refraction coexist in this kind of metasurface, the efficiency of this metasurface is very low. Pancharatnam–Berry-phase metasurface is also known as geometric phase metasurface. A complete phase can be achieved easily by varying the orientation angle of the unit cell. Therefore, this kind of metasurface can be designed and fabricated easily. However, this type of metasurface has a limitation to circularly polarized light operation. As compared to the above two metasurfaces, Huygens' metasurface based on the surface equivalence principle has a very high transmission efficiency in the microwave frequency. But the Huygens' metasurface has a big volume since it consists of multi-layered unit cells.[65] In addition, the Huygens' metasurface in optical regime still has a low efficiency due to weak magnetic response of natural materials and metallic loss in this high frequency band.[172] In order to enhance the efficiency in optical regime, all-dielectric metasurface composed of high refractive-index dielectric nanoparticles has been proposed.[173–176] However, the material choice of all-dielectric metasurface is few.[177] Besides the design and fabrication of metasurfaces, metasurfaces-based devices have also constantly being proposed in recent years. Although great progress has been made in metasurfaces, a broadband metasurface with high efficiency and tunable is still a challenge. Because of the peculiar behavior of metasurfaces, metasurfaces will remain a research hotspot in the scientific field in the next few years.

## Acknowledgment

In this manuscript, we summarize our group's work on metamaterials and metasurfaces. So we thank the contributions of all of our group members. Professor Xiaopeng Zhao conceives the idea, and Dr Yahong Liu writes the manuscript.

## References

[1] Veselago V G 1968 *Sov. Phys. Usp.* **10** 509
[2] Veselago V G and Narimanov E E 2006 *Nat. Mater.* **5** 759
[3] Pendry J B, Holden A J and Stewart W J 1996 *Phys. Rev. Lett.* **76** 4773
[4] Pendry J B, Holden A J, Robbins D J and Stewart W J 1999 *IEEE Trans. Microwave Theor. Techniq.* **47** 2075
[5] Shelby R A, Smith D R and Schultz S 2001 *Science* **292** 77
[6] Pendry J B 2000 *Phys. Rev. Lett.* **85** 3966
[7] Schurig D, Mock J J, Justice B J, Cummer S A, Pendry J B, Starr A F and Smith D R 2006 *Science* **314** 977
[8] Ma H F and Cui T J 2010 *Nat. Commun.* **1** 21
[9] Kafesaki M, Tsiapa I, Katsarakis N, Koschny T, Soukoulis C M and Economou E N 2007 *Phys. Rev. B* **75** 235114
[10] Liu Y, Luo C and Zhao X 2007 *Acta Phys. Sin.* **56** 5883 (in Chinese)
[11] Wang D, Ran L, Chen H, Mu M, Kong J A and Wu B I 2007 *Appl. Phys. Lett.* **90** 254103
[12] Aydin K, Li Z F, Hudlicka M, Tretyakov S A and Ozbay E 2007 *New J. Phys.* **9** 326
[13] Zhao X, Zhao Q, Zhang F, Zhao W and Liu Y 2006 *Chin. Phys. Lett.* **23** 99
[14] Yao Y and Zhao X 2007 *J. Appl. Phys.* **101** 124904
[15] Zhou X and Zhao X 2007 *Appl. Phys. Lett.* **91** 181908
[16] Zhu W, Zhao X and Guo J 2008 *Appl. Phys. Lett.* **92** 241116
[17] Liu B, Zhao X, Zhu W, Luo W and Cheng X 2008 *Adv. Funct. Mater.* **18** 3523
[18] Zhang S, Fan W, Malloy K J, Brueck S R, Panoiu N C and Osgood R M 2005 *Opt. Express* **13** 4922
[19] Yuan Y, Bingham C, Tyler T, Palit S, H, T H, Padilla W J, Smith D R, Jokerst N M and Cummer S A 2008 *Opt. Express* **16** 9746
[20] Valentine J, Zhang S, Zentgraf T, Ulin-Avila E Genov D A, Bartal G and Zhang X 2008 *Nature* **455** 376
[21] Dolling G, Enkrich C, Wegener M, Zhou J F, Soukoulis C M and Linden S 2005 *Opt. Lett.* **30** 3198
[22] Zhao Q, Kang L, Du B, Zhao H, Xie Q, Huang X, Li B, Zhou J and Li L 2008 *Phys. Rev. Lett.* **101** 027402
[23] Peng L, Ran L, Chen H, Kong J A and Grzegorczyk T M 2007 *Phys. Rev. Lett.* **98** 157403
[24] Ginn J C and Brener I 2012 *Phys. Rev. Lett.* **108** 097402
[25] Liu H, Zhao X, Yang Y, Li Q and Lv J 2008 *Adv. Mater.* **20** 2050
[26] Shalaev V M, Cai W, Chettiar U K, Yuan H, Sarychev A K, Drachev V P and Kildishev A V 2005 *Opt. Lett.* **30** 3356
[27] Cheng X, Chen H, Jiang T, Ran L and Kong J A 2008 *Appl. Phys. Lett.* **92** 174103
[28] Tsakmakidis K L, Boardman A D and Hess O 2007 *Nature* **450** 397
[29] Kim E and Shen Y R 2007 *Appl. Phys. Lett.* **91** 173105
[30] Zhu J, Hao T, Stevens C J and Edwards D J 2008 *Appl. Phys. Lett.* **93** 234105
[31] Bulu I, Caglayan H and Ozbay E 2005 *Opt. Express* **13** 10238
[32] Hsu Y J, Huang Y C, Lih J S and Chern J L 2004 *J. Appl. Phys.* **96** 1979
[33] Gokkavas M, Guven K, Bulu I, Aydin K, Penciu R S, Kafesaki M, Soukoulis C M and Ozbay E 2006 *Phys. Rev. B* **73** 193103
[34] Pimenov A, Loidl A, Gehrke K, Moshnyaga V and Samwer K 2007 *Phys. Rev. Lett.* **98** 197401
[35] Cui T J, Hao Z, Yin X X, Hong W and Kong J A 2004 *Phys. Lett. A* **323** 484
[36] Simovski C R and Sauviac B 2004 *Phys. Rev. E* **70** 046607
[37] Ozbay E, Aydin K, Cubukcu E and Bayindir M 2003 *IEEE Trans. Antennas Propagat.* **51** 2592

[38] Grzegorczyk T M, Moss C D, Lu J, Chen X, Pacheco J and Kong J A 2005 *IEEE Trans. Microw. Theory Tech.* **53** 2956

[39] Katsarakis N, Koschny T, Kafesaki M, Economou E N, Ozbay E and Soukoulis C M 2004 *Phys. Rev. B* **70** 201101

[40] Tretyakov S, Nefedov I, Sihvola A, Maslovski S and Simovski C 2003 *J. Electromagnetic Wave.* **17** 695

[41] Pendry J B 2004 *Science* **306** 1353

[42] Singh R, Plum E, Zhang W and Zheludev N I 2010 *Opt. Express* **18** 13425

[43] Zhang Y, Jin W, Dong X, Zhao Z and Duan X 2012 *Opt. Express* **20** 10776

[44] Kwon D H , Werner P L and Werner D H 2008 *Opt. Express* **16** 11802

[45] Saba M, Thiel M, Turner M D, Hybe S T, Gu M, Grossw-Brauckmann K, Neshev D N, Mecke K and Schröder-Turk G E 2011 *Phys. Rev. Lett.* **106** 103902

[46] Zhao R, Koschny T, Economou E N and Soukoulis C M 2011 *Phys. Rev. B* **83** 075108

[47] Rogacheva A V, Fedotov V A Schwanecke A S and Zheludev N I 2006 *Phys. Rev. Lett.* **97** 177401

[48] Zarifi D, Oraizi H and Soleimani M 2012 *Prog. Electromagn. Res.* **123** 337

[49] Grady N K, Heyes J E, Chowdhury D R, Zeng Y, Reiten M T, Azad A K, Taylor A J, Dalvit D A R and Chen H T 2013 *Science* **340** 1304

[50] Song K, Zhao X, Fu Q, Liu Y and Zhu W 2012 *Electromagn. Waves Appl.* **26** 1967

[51] Song K, Liu Y, Fu Q, Zhao X, Luo C and Zhu W 2013 *Opt. Express* **21** 7439

[52] Song K, Ding C, Su Z, Liu Y, Luo C, Zhao X, Bhattarai K and Zhou J 2016 *J. Appl. Phys.* **120** 245102

[53] Song K, Su Z, Wang M, Silva S, Bhattarai K, Ding C, Liu Y, Luo C, Zhao X and Zhou J 2017 *Sci. Rep.* **7** 10730

[54] Song K, Zhao X P, Liu Y H, Fu Q H and Luo C R 2013 *Appl. Phys. Lett.* **103** 101908

[55] Liu Y, Guo Q, Liu H, Liu C, Song K, Yang B, Hou Q, Zhao X, Zhang S and NavarroC ía M 2018 *Phys. Rev. Appl.* **9** 054033

[56] Liu Y, Luo Y, Liu C, Song K and Zhao X 2017 *Appl. Phys. A* **123** 571

[57] Liu Y, Song K, Qi Y, Gu S and Zhao X 2013 *IEEE Antennas Wireless Propag. Lett.* **12** 1359

[58] Kildishev A V, Boltasseva A and Shalaev V M 2013 *Science* **339** 1232009

[59] Yu N, Genevet P, Kats M A, Aieta F, Tetienne J, Capasso F and Gaburro Z 2011 *Science* **334** 333

[60] Pfeiffer C and Grbic A 2013 *Appl. Phys. Lett.* **102** 231116

[61] Zhao Y, Belkin M A and Alù A 2012 *Nat. Commun.* **3** 870

[62] Zhang P, Hu Y, Li T, Cannan D, Yin X, Morandotti R, Chen Z and Zhang X 2012 *Phys. Rev. Lett.* **109** 193901

[63] Li Y, Cai B, Cheng Q and Cui T J 2015 *J. Phys. D: Appl. Phys.* **48** 035107

[64] Sun S, He Q, Xiao S, Xu Q, Li X and Zhou L 2012 *Nat. Mater.* **11** 426

[65] Pfeiffer C and Grbic A 2013 *Phys. Rev. Lett.* **110** 197401

[66] Ra'di Y, Sounas D L and Alù A 2017 *Phy. Rev. Lett.* **119** 067404

[67] Lin B Q, Guo J X, Huang B G, Fang L B, Chu P and Liu X W 2018 *Chin. Phys. B* **27** 054204

[68] Gao X J, Zhu L and Guo W L 2017 *Acta Phys. Sin.* **66** 204102 (in Chinese)

Gao X J, Zhu L and Guo W L 2017 *Acta Phys. Sin.* **66** 204102 (in Chinese)

[69] Khan M I and Tahir F A 2018 *Chin. Phys. B* **27** 014101

[70] Hou H S, Wang G M, Li H P, Guo W L, Li T J and Cai T 2017 *Chin. Phys. B* **26** 057701

[71] Odit M, Kapitanova P, Alaee P, Rockstuhl C and Kivshar Y S 2016 *Appl. Phys. Lett.* **108** 221903

[72] Caligiuri V, De Sio L, Petti L, Capasso R, Rippa M, Maglione M G, Tabiryan N and Umeton C 2014 *Adv. Opt. Mater.* **2** 950

[73] Guo R, Rusak E, Staude E, Dominguez J, Decker M, Rockstuhl C, Brener I, Neshev D N and Kivshar Y S 2016 *ACS Photon.* **3** 349

[74] Zhan A, Colburn S, Trivedi R, Fryett T K, Dodson C M and Majumdar A 2016 *ACS Photon.* **3** 209

[75] Ma Z, Hanham S M, Albella P, Ng B, Lu H T, Gong Y, Maier S A and Hong M 2016 *ACS Photon.* **3** 1010

[76] Liu Y, Liu C, Song K, Li M and Zhao X 2018 *J. Phys. D: Appl. Phys.* **51** 095103

[77] Cole M A, Powell D A and Shadrivov I V 2016 *Nanotechnology* **27** 424003

[78] Kang M, Liu F, Li T F, Guo Q H , Li J and Chen J 2013 *Opt. Lett.* **38** 3086

[79] Song Q H, Zhang W, Wu P C, Zhu W, Shen Z X, Chong P H J, Liang Q X, Yang Z C, Hao L Y, Cai H, Zhou H F, Gu Y, Lo G Q , Tsai D P, Bourouina T, Leprince-Wang Y and Liu A Q 2017 *Adv. Opt. Mater.* **5** 1601103

[80] Yoo M and Lim S 2014 *Appl. Phys. Express* **7** 112204

[81] Li T J, Liang J G, Li H P, Niu X B and Liu Y Q 2017 *Acta Phys. Sin.* **66** 064102 (in Chinese)

[82] Liu K, Wang G, Cai T, Guo W, Zhuang Y and Liu G 2018 *Chin. Phys. B* **27** 084101

[83] Cheng H, Wei X, Yu P, Li Z, Liu Z, Li J, Chen S and Tian J 2017 *Appl. Phys. Lett.* **110** 171903

[84] Wan X, Jiang W X, Ma H F and Cui T J 2014 *Appl. Phys. Lett.* **104** 151601

[85] Chen P Y , Argyropoulos C and Alu A 2013 *Phys. Rev. Lett.* **111** 233001

[86] Germain D, Seetharamdoo D, Burokur S N and Lustrac A 2013 *Appl. Phys. Lett.* **103** 124102

[87] Liu Y and Zhao X 2008 *IET Microw. Antennas Propag.* **2** 737

[88] Liu Y and Zhao X 2011 *Microw. Opt. Technol. Lett.* **53** 1945

[89] Liu Y and Zhao X 2009 *Microw. Opt. Technol. Lett.* **51** 1732

[90] Liu Y, Guo X, Gu S and Zhao X 2013 *Inter. J. Antennas Propag.* **2013** 215681

[91] Liu Y and Zhao X 2014 *IEEE Antennas Wireless Propag. Lett.* **13** 1473

[92] Liu Y, Zhou X, Zhu Z and Zhao X 2016 *J. Phys. D: Appl. Phys.* **49** 075107

[93] Liu Y, Jin X, Zhou X, Luo Y, Song K, Huang L and Zhao X 2016 *J. Phys. D: Appl. Phys.* **49** 405304

[94] Liu Y, Gu H and Zhao X 2011 *IEEE Antennas Wireless Propag. Lett.* **10** 658

[95] Tang H, Hou Q, Liu Y and Zhao X 2013 *Int. J. Antennas. Propag.* **2013** 575062

[96] Hou Q, Tang H, Liu Y and Zhao X 2012 *IEEE Antennas Wireless Propag. Lett.* **11** 442

[97] Hou Q, Tang H, Liu Y and Zhao X 2013 *Microw. Opt. Techn. Lett.* **55** 2393

[98] Hou Q, Li C, Sun G and Zhao X 2016 *IEEE Trans. Antennas Propag.* **64** 3717

[99] Huang L, Chen X, Muhlenbernd H, Li G, Bai B, Tan Q, Jin G, Zentgraf T and Zhang S 2012 *Nano Lett.* **12** 5750

[100] Pfeiffer C and Grbic A 2013 *IEEE Trans. Microw. Theory Tech.* **61** 4407

[101] Huang L, Chen X, Mu¨hlenbernd H, Zhang H, Chen S, Bai B, Tan Q, Jin G, Cheah K W , Qiu C W , Li J, Zentgraf T and Zhang S 2013 *Nat. Commun.* **4** 2808

[102] Shaltout A, Liu J, Shalaev V M and Kildishev A V 2014 *Nano Lett.* **14** 4426

[103] Wan X, Li Y B, Cai B G and Cui T J 2014 *Appl. Phys. Lett.* **105** 121603

[104] Pfeiffer C, Zhang C, Ray V, Guo L J and Grbic A 2014 *Phys. Rev. Lett.* **113** 023902

[105] Li Z, Palacios E, Butun S and Aydin K 2015 *Nano Lett.* **15** 1615

[106] Zhang Y, Zhou L, Li J, Wang Q and Huang C 2015 *Sci. Rep.* **5** 10119

[107] Falco A D, Zhao Y and Alú A 2011 *Appl. Phys. Lett.* **99** 163110

[108] Decker M, Kremers C, Minovich A, Staude I, Miroshnichenko A E, Chigrin D, Neshev D N, Jagadish C and Kivshar Y S 2013 *Opt. Express* **21** 8879

[109] Wan X, Shen X P and Cui T J 2013 *Opt. Express* **21** 17531

[110] Yin X, Ye Z, Rho J, Wang Y and Zhang X 2013 *Science* **339** 1405

[111] Ni X, Ishii S, Kildishev A V and Shalaev V M 2013 *Light-Sci. Appl.* **2** e72

[112] Huang L, Chen X, Bai B, Tan Q, Jin G, Zentgraf T and Zhang S 2013 *Light-Sci. Appl.* **2** e70

[113] Kang M, Zhang H, Zhang X, Yang Q, Zhang W and Han J 2018 *Phys. Rev. Appl.* **9** 054018

[114] Tang B, Li Z, Palacios E, Liu Z, Butun S and Aydin K 2017 *IEEE Photonic. Tech. Lett.* **29** 295

[115] Yazdi M, Albooyeh M, Alaee R, Asadchy V, Komjani N, Rockstuhl C, Simovski C R and Tretyakov S 2015 *IEEE Trans. Antennas Propag.* **63** 3004

[116] Matsuno Y and Sakurai A 2017 *Opt. Mater. Express* **7** 618
[117] Yu N, Aieta F, Genevet P, Kats M A, Gaburro Z and Capasso F 2012 *Nano Lett.* **12** 6328
[118] Li Y, Zhang J, Qu S, Wang J, Chen H, Zheng L, Xu Z and Zhang A 2014 *J. Phys. D: Appl. Phys.* **47** 425103
[119] Zhang F L, Zhao Q, Liu Y H, Luo C R and Zhao X P 2004 *Chin. Phys. Lett.* **21** 1330
[120] Kang L, Luo C, Zhao Q, Song J, Fu Q and Zhao X 2004 *Chin. Sci. Bull.* **49** 2440
[121] Song J, Zhao W, Fu Q and Zhao X 2007 *J. Appl. Phys.* **101** 023702
[122] Zhu W, Zhao X and Ji N 2007 *Appl. Phys. Lett.* **90** 011911
[123] Zhao X P, Zhao Q, Kang L, Song J and Fu Q H 2005 *Phys. Lett. A* **346** 87
[124] Zhou X, Liu Y and Zhao X 2010 *Appl. Phys. A* **98** 643
[125] Zhou X, Zhao X P and Liu Y 2008 *Opt. Express* **16** 7674
[126] Zhu W and Zhao X 2009 *J. Appl. Phys.* **106** 093511
[127] Zhou X, Fu Q H, Zhao J, Yang Y and Zhao X P 2006 *Opt. Express* **14** 7188
[128] Luo C R, Kang L, Zhao Q, Fu Q H, Song J and Zhao X P 2005 *Acta Phys. Sin.* **54** 1607 (in Chinese)
[129] Zhao Q, Zhao X P, Kang L, Zhang F L, Liu Y H and Luo C R 2004 *Acta Phys. Sin.* **53** 2206 (in Chinese)
[130] Liu Y, Zhou X, Song K, Gu S, Liu Z, Guo L and Zhao X 2014 *Appl. Phys. Lett.* **105** 201911
[131] Fedotov V A, Mladyonov P L, Prosvirnin S L, Rogacheva A V, Chen Y and Zheludev N I 2006 *Phys. Rev. Lett.* **97** 167401
[132] Wu L, Yang Z, Cheng Y, Zhao M, Gong R, Zheng Y, Duan J and Yuan X 2013 *Appl. Phys. Lett.* **103** 021903
[133] Mutlu M, Akosman A E, Serebryannikov A E and Ozbay E 2011 *Opt. Express* **19** 14290
[134] Cheng Y, Nie Y, Cheng Z and Gong R 2014 *Prog. Electromagn. Res.* **145** 263
[135] Liu Y, Zhou X, Song K, Wang M and Zhao X 2015 *J. Phys. D: Appl. Phys.* **48** 365301
[136] Liu Y, Liu C, Jin X, Zhang B, Zhang Y, Zhu X, Su B and Zhao X 2018 *Microw. Opt. Technol. Lett.* **60** 330
[137] Liu Y, Jin X, Luo Y, Song K and Zhao X 2017 *Plasmonics* **12** 1431
[138] Sun G, Chen H, Cheng S and Zhao X 2017 *Physica B* **525** 127
[139] Zhu W and Zhao X 2009 *J. Opt. Soc. Am. B* **26** 2382
[140] Bao S, Luo C R and Zhang Y P and Zhao X P 2010 *Acta Phys. Sin.* **59** 3187 (in Chinese)
[141] Gu S, Su B and Zhao X 2013 *J. Appl. Phys.* **114** 163702
[142] Wang B, Gong B, Wang M, Weng B and Zhao X 2015 *Appl. Phys. A* **118** 1559
[143] Gu S, Barrett J P, H, T H, Popa B I and Cummer S A 2010 *J. Appl. Phys.* **108** 064913
[144] Zhu W R , Zhao X P , Bao S and Zhang Y P 2010 *Chin. Phys. Lett.* **27** 014204
[145] Liu Y, Gu S, Luo C and Zhao X 2012 *Appl. Phys. A* **108** 19
[146] Oliner A A 2003 *IEEE MTT-S Digest* **191**
[147] Eleftheriades G V, Iyer A K and Kremer P C 2002 *IEEE Trans. Microwave Theory Tech.* **50** 2702
[148] Sanada A, Caloz C and Itoh T 2004 *IEEE Trans. Microwave Theory Tech.* **52** 1252
[149] Grbic A and Eleftheriades G V 2002 *J. Appl. Phys.* **92** 5930
[150] Grbic A and Eleftheriades G V 2004 *Phys. Rev. Lett.* **92** 117403
[151] Lai A, Leong K M K H and Itoh T 2007 *IEEE Trans. Antennas Propag.* **55** 868
[152] Casares-Miranda F P, Camacho-Peñalosa C and Caloz C 2006 *IEEE Trans. Antennas Propag.* **54** 2292
[153] Rajab K, Mittra R and Lanagan M T 2007 *IET Microw. Antennas Propag.* **1** 39
[154] Jie X, Luo C and Zhao X 2008 *Microw. Opt. Technol. Lett.* **50** 767
[155] Eleftheriades G V and Balmain K G 2005 *Negative-Refraction Metamaterials: Fundamental Principles and Applications* (New York: Wiley)
[156] Caloz C and Itoh T 2013 *Mat. Sci. Eng. B* **178** 1285
[157] Antoniades M A and Eleftheriades G V 2009 *IEEE Antennas Wireless Propag. Lett.* **8** 258
[158] Park J H, Ryu Y H, Lee J G and Lee J H 2007 *IEEE Trans. Antennas Propag.* **55** 3710
[159] Lee C J, Leong K M K H and Itoh T 2006 *IEEE Trans. Antennas Propag.* **54** 2283
[160] Borja A L, Hall P S, Liu Q and Iizuka H 2007 *IEEE Antennas Wireless Propag. Lett.* **6** 495
[161] Jie X, Luo C, Liu Y, Tang H and Zhao X 2011 *Microw. Opt. Technol. Lett.* **53** 300
[162] Chen H, Wu B I, Ran L, Grzegorczyk T M and Kong J A 2006 *Appl. Phys. Lett.* **89** 053509
[163] Dhouibi A, Burokur S N and Lustrac A 2014 *J. Appl. Phys.* **115** 194901
[164] Pacheco-Pena V, Torres V, Orazbayev B, Beruete M, Navarro-Cia M, Sorolla M and Engheta N 2014 *Appl. Phys. Lett.* **105** 243503
[165] Sajuyigbe S, Ross M, Geren P, Cummer A, Tanielian M H and Smith D R 2010 *IET Microw. Antennas Propag.* **4** 1063
[166] Ma H F, Chen X, Yang X M, Jiang W X and Cui T J 2010 *J. Appl. Phys.* **107** 014902
[167] Xu H X , Wang G M , Qi M Q and Xu Z M 2012 *Appl. Phys. Lett.* **101** 173501
[168] Blanchard R, Aoust G, Genevet P, Yu N, Kats M A, Gaburro Z and Capasso F 2012 *Phys. Rev. B* **85** 155457
[169] Jiang S C , Xiong X, Hu Y S , Jiang S W , Hu Y H , Xu D H , Peng R W and Wang M 2015 *Phys. Rev. B* **91** 125421
[170] Kenney M, Li S, Zhang X, Su X, Kim T, Wang D, Wu D, Ouyang C, Han J, Zhang W, Sun H and Zhang S 2016 *Adv. Mater.* **28** 9567
[171] Monticone F, Estakhri N M and Alù A 2013 *Phys. Rev. Lett.* **110** 203903
[172] Pfeiffer C, Emani N K, Shaltout A M, Boltasseva A, Shalaev V M and Grbic A 2014 *Nano Lett.* **14** 2491
[173] Kruk S, Hopkins B, Kravchenko I I, Miroshnichenko A, Neshev D N and Kivshar Y S 2016 *APL Photon.* **1** 030801
[174] Iyer P P, Butakov N A and Schuller J A 2015 *ACS Photon.* **2** 1077
[175] Kuznetsov A I, Miroshnichenko A E, Brongersma M L, Kivshar Y S and Luk'yanchuk B 2016 *Science* **354** 6314
[176] Yu Y F, Zhu A Y, Paniagua-Domínguez R, Fu Y H, Luk'yanchuk B and Kuznetsov A I 2015 *Laser Photon. Rev.* **9** 412
[177] Hsiao H H , Chu C H and Tsai D P 2017 *Small Methods* **1** 1600064